CONTENTS

The Frequency of Annealing Twins in FCC Iron–Nickel–Chromium Alloys
R. L. Cowan, R. W. Staehle 3
Effect of Sulfur on the Fatigue Behavior of Bearing Steel
C. M. Lyne, A. Kasak 10
Structure and Properties of Fe–Ni–Co–Ti Maraging Steel
I-Lin Cheng, G. Thomas 14
Effects of Repeated Thermal Cycling on the Microstructure of 300-Grade Maraging Steel
Alfred Goldberg 26
The Determination of Strain Distribution Across the Interior of a Specimen From Measurements of Local Changes in Grain Shape
John E. Flinn, Elliott M. Philofsky 37
Observations on Micromechanisms of Fatigue-Crack Propagation in 2024 Aluminum
D. A. Meyn 42
The Nature of Fatigue-Crack Propagation in Air and Vacuum for 2024 Aluminum
D. A. Meyn 52
A Study of Austenite Reversion During Aging of Maraging Steels
D. T. Peters 62
Heat Treatment of a Cr–Mo–Co Martensitic Stainless Steel for Optimum Combinations of Strength, Toughness and Stress-Corrosion Resistance
R. T. Ault, R. B. Holtmann, J. R. Myers 75
Properties of Stainless Steels With a Microduplex Structure
R. C. Gibson, H. W. Hayden, J. H. Brophy 85
Discussion 640
Application of a Method of Estimating High-Temperature Low-Cycle Fatigue Behavior of Materials
G. R. Halford, S. S. Manson 94
Role of Phosphorus in $M_{23}C_6$ Precipitation in an Austenitic Stainless Steel
B. R. Banerjee, E. J. Dulis, J. J. Hauser 103
Decarburization of Alloy Steels
Hiroshi Oikawa, J.-F. Remy, A. G. Guy 110
Effect of Microstructure on the Fracture Properties of Titanium Alloys in Air and Salt Solution
R. E. Curtis, W. F. Spurr 115
The Structure and Development of Fatigue Striations in Al
E. Levine, S. Weissmann 128
Carbide and Intermetallic Instability in Advanced Nickel-Base Superalloys
H. E. Collins, R. J. Quigg 139
Low-Cycle Fatigue of Udimet 700 at 1700 F
C. H. Wells, C. P. Sullivan 149
The Fracture Behavior of Spheroidized Carbon Steels
C. T. Liu, J. Gurland 156
Cyclic Transformation in Fe–Ni–C Alloys
B. Hyatt, G. Krauss 168
Stress Relaxation and Cyclic Hardening of 12Ni–5Cr–3Mo Maraging Steel During Low-Cycle Fatigue
R. W. Hinton 176
Some Observations on Dimple Size in Cyclic-Load-Induced Plane-Stress Fracture (TN)*
W. W. Gerberich, C. E. Hartbower 184
Strength and Toughness Properties of a Cold Rolled Low-Silicon Stainless Steel (TN)
S. Floreen 188
Transverse Sectioning of Field Ion Microscope Specimens for Transmission Electron Microscopy (TN)
R. D. French, M. H. Richman 190

* The notation TN appearing in parentheses designates a Technical Note.

Correction to Vol. 60, p. 707 192
Use of Electron Microautoradiography for Evaluating Microsegregation of Hydrogen in Titanium Alloys
N. A. Tiner, T. L. Mackay, S. K. Asunmaa, R. G. Ingersoll 195
Correlation of Structural and Mechanical Anisotropy in Rolled Ductile Iron
K. D. Sheffler, J. F. Libsch 203
The Initiation of Fatigue Microcracks Under Sequential Bending and Torsional Loads
J. A. Bennett 210
The Effect of Lead on the Mechanical Properties of 4145 Steel
S. Mostovoy, N. N. Breyer 219
X-Ray Study of the Aging Process in an Austenitic Fe–31Ni–3.5Ti Alloy
J. K. Abraham, J. K. Jackson, L. Leonard 233
The Structure Sensitivity of the Effects of Pressure upon the Ductility of Fe-C Materials
T. E. Davidson, G. S. Ansell 242
Columbium Carbonitride Precipitation in Low-Alloy Steels With Particular Emphasis on "Precipitate-Row" Formation
J. M. Gray, R. B. G. Yeo 255
Discussion 851
Intergranular Corrosion and Mechanical Properties of Austenitic Stainless Steels
K. T. Aust, J. S. Armijo, E. F. Koch, J. H. Westbrook 270
The Separation of Gamma Prime From Udimet 700
Owen H. Kriege, C. P. Sullivan 278
Some Characteristics of Aqueous Stress-Corrosion in Titanium Alloys
D. N. Fager, W. F. Spurr 283
Discussion 850
Microcracking in Fe-C Acicular Martensite
A. R. Marder, A. O. Benscoter 293
Superplasticity in Lead-Tin Alloys
S. W. Zehr, W. A. Backofen 300
Calculation of Interdiffusion Coefficients Considering Variations in Atomic Volume
A. G. Guy, R. T. DeHoff, C. B. Smith 314
Effect of Cold Work Upon the Embrittlement of 70:30 Alpha-Brass in 2% Na Amalgam
J. V. Rinnovatore, J. D. Corrie, J. D. Meakin 321
Supersaturation in Rapidly Quenched Al-Rich Al-Si Alloys
Motoo Itagaki, Bill C. Giessen, Nicholas J. Grant 330
Tensile Properties of Gamma Quenched and Aged Uranium-Base Niobium Alloys
Ross J. Jackson, Delmar V. Miley 336
A Fractographic Feature of Plane-Strain Fracture in 0.45C–Ni–Cr–Mo Steel (TN)
W. A. Spitzig 344
A Sensitive Metallographic Method for Detecting Austenite Formation in Low Carbon Steels (TN)
H. I. Aaronson, T. L. Johnston, D. J. Schmatz 349
The Effect of Refractory Elements on the Stability of Complex Carbides in Ni-Base Superalloys (TN)
R. L. Dreshfield 352
Diffusion of Zn^{65} in Copper-Rich Solid Solutions of the Cu-Ni-Zn System (TN)
Hiroshi Oikawa, K. J. Anusavice, R. T. DeHoff, A. G. Guy 354
Discussion of "A Theoretical Explanation for the Increase in Fatigue Strength of Mild Steel at Elevated Temperatures" (Vol. 60, 1967, p. 707) 357
Metallurgical Classics:
Heat Treatment and Constitution of Duralumin
Explanatory Note 365
Commentary: Conception of the Precipitation Mechanism of Age Hardening
John B. Newkirk 367
Heat Treatment and Constitution of Duralumin
P. D. Merica, R. G. Waltenberg, H. Scott 381
Superplasticity of Low-Alloy Steels
W. B. Morrison 423

Lanthanum-Lead System
O. D. McMasters, S. D. Soderquist, K. A. Gschneider, Jr. 435
The Dependence of Fatigue-Crack Growth Rate on the Stress Intensity Factor and the Mechanical Properties of Some High-Strength Steels
G. A. Miller 442
Effect of Dissolved Oxygen and NaCl on Corrosion Fatigue of 0.18% Carbon Steel
D. J. Duquette, H. H. Uhlig 449
A Microstructural Study of the Role of Vanadium in Decreasing the Toughness of 0.5% Mo-B Steels
G. H. Karchner, E. T. Stephenson 457
Factors Influencing the Path of Stress-Corrosion Cracking in Alpha-Phase Copper Alloys Exposed to Aqueous Ammonia Environments
E. N. Pugh, J. V. Craig, W. G. Montague 468
The Deformation and Fracture of Stainless Steels Having Microduplex Structures
H. W. Hayden, S. Floreen 474
The Influence of Austenite and Ferrite on the Mechanical Properties of Two-Phase Stainless Steels Having Microduplex Structures
S. Floreen, H. W. Hayden 489
Morphology of Fracture in Pearlite
U. Lindborg 500
Age Hardening of Magnesium Alloy LA141A (Mg + 14 wt % Li + 1 wt % Al)
John C. McDonald 505
Fringe Contrast at Coherent Precipitate Interfaces in a Nickel-Base Alloy
J. M. Oblak, B. H. Kear 519
Determining Recovery in Cold Reduced Low-Carbon Steel Strip
P. N. Richards, J. D. Russell, A. P. Tomlinson 528
Tensile Fracture Criteria for a Mild Steel
D. P. Clausing 534
The Interrelation of Grain Size and Superplastic Deformation in Ni–Cr–Fe Alloys
H. W. Hayden, J. H. Brophy 542
Discussion 852
Mechanical Properties of Al-B Composites
K. C. Antony, W. H. Chang 550
Strain Hardening and Recovery in Superplastic Pb–5% Cd
Thomas H. Alden 559
Fatigue Crack Propagation and Plane Strain Fracture Toughness Characteristics of a 9Ni–4Co–0.25C Steel
T. W. Crooker, L. A. Cooley, E. A. Lange, C. N. Freed 568
The Sulfide Phases in Iron-Chromium Steels
C. W. Kovach, R. G. Wells, A. Moskowitz 575
Potentiostatically Controlled Etching of Nickel-Aluminum Alloys
C. P. Sullivan, J. Jensen, D. S. Duvall, T. T. Field 582
Volume Fraction Analysis of Phases in Textured Alloys
R. L. Miller 592
Continuous Observation of the Sintering of Silver Particles in the Electron Microscope
G. H. Gessinger, F. V. Lenel, G. S. Ansell 598
Widmanstätten Ferrite Formation in Fe-C Alloys
R. D. Townsend, J. S. Kirkaldy 605
Contour Plot of Elastic Modulii for Cubic Crystals in the Stereographic Triangle (TN)
P. S. Venkatesan 620
Continuous-Cooling Transformation Diagrams of Ti–8Al–1Mo–1V (TN)
K. C. Wu 621
Failure of Alpha Titanium in Methanol-Hydrochloric Acid-Water Solutions (TN)
A. J. Sedriks, P. W. Slattery, J. A. S. Green 625
A Microfractographic Investigation of Fatigue Cracks in a Low Alloy Cast Steel (TN)
Hans Nordberg, Bertil Aronsson 627

Cerium Diffusion in Delta Stabilized Pu-Ce Alloys (TN)
M. R. Harvey, A. L. Rafalski, D. H. Riefenberg 629
The Effect of Carbon on the M_s Temperature of a 14Cr–4Ni Iron Alloy (TN)
E. Snape, F. W. Schaller 631
Structure and Strengthening Mechanisms in 300-Grade 18Ni–Co–Mo–Ti Maraging Steel (TN)
W. A. Spitzig, J. M. Chilton, C. J. Barton 635
Symposium on Dislocation Climb and High-Temperature Creep Processes
Abstracts 642
Campbell Memorial Lecture:
Sheet Steel—Micrometallurgy by the Millions
Donald J. Blickwede 651
Symposium on Dislocation Climb and High-Temperature Creep Processes 680
Keynote Paper:
Dislocation Climb Theory of Steady-State Creep
J. Weertman 681
Abstracts of Invited Oral Presentations 695
Interdiffusion Between Nickel and Uranium
G. Kimmel, A. Bar-Or, A. Rosen 703
Development of a Nickel-Base Superalloy Using Statistically Designed Experiments
H. E. Collins, R. J. Quigg, R. L. Dreshfield 711
The Deformation of Wrought Zn–Ni–Ti Alloys
N. R. Risebrough, J. A. Lund 722
Electrical Resistivity Anomaly in Nickel-Base Alloys
H. E. McCoy, Jr., D. L. McElroy 730
Ductility of Textured Zircaloy-2
D. Lee 742
An Analysis of Microstructural Changes in 52100 Steel Bearings During Cyclic Stressing
J. Buchwald, R. W. Heckel 750
Elastic Springback and Residual Stresses in Sheet Metal Formed by Bending
Carl A. Queener, R. J. DeAngelis 757
The Fatigue Characteristics of Unidirectionally Solidified Al–Al_3Ni Eutectic Alloy
W. R. Hoover, R. W. Hertzberg 769
A Field Ion Microscope Investigation of the Effect of Rhenium on the Lattice Solid Solubility of Oxygen in Tungsten
D. T. Novick, E. S. Machlin 777
Precipitation in Quenched and Aged Beryllium Ingot Sheet
F. J. Fraikor, A. W. Brewer 784
The Conditioning of Retained Austenite in High Speed Steel
R. J. Beltz, R. W. Lindsay 790
18% Nickel 350 Maraging Steel
G. W. Tuffnell, R. L. Cairns 798
Slip-Induced Crack Formation in Mild Steel
A. R. Rosenfield, E. Votava, G. T. Hahn 807
Increasing the Toughness of the Martensitic Stainless Steel AFC 77 by Control of Retained Austenite, Ausforming, and Strain Aging
D. Webster 816
Substructure Strengthening in Aluminum
J. S. H. Lake, G. B. Craig 829
Relationship Between Microstructures and Mechanical Properties on Tempering a Mo–W–V Alloy Steel
Charles R. Simcoe, A. E. Nehrenberg, V. Biss, A. P. Coldren 834
Preliminary Toughness Results on TRIP Steel (TN)
W. W. Gerberich, P. L. Hemmings, M. D. Merz, V. F. Zackay 843
Grain Size Refinement of Ingot Beryllium by Straining Under Hydrostatic Pressure (TN)
N. Inoue, H. Conrad 847

Corrections to Vol. 61, pp. 8 and 629 853
Metallurgical Classics:
The Phenomena of Rupture and Flow in Solids
Explanatory Note 859
Commentary: Griffith's Crack Theory
JOHN J. GILMAN 861
The Phenomena of Rupture and Flow in Solids
A. A. GRIFFITH 871
Index to Volume 61 907

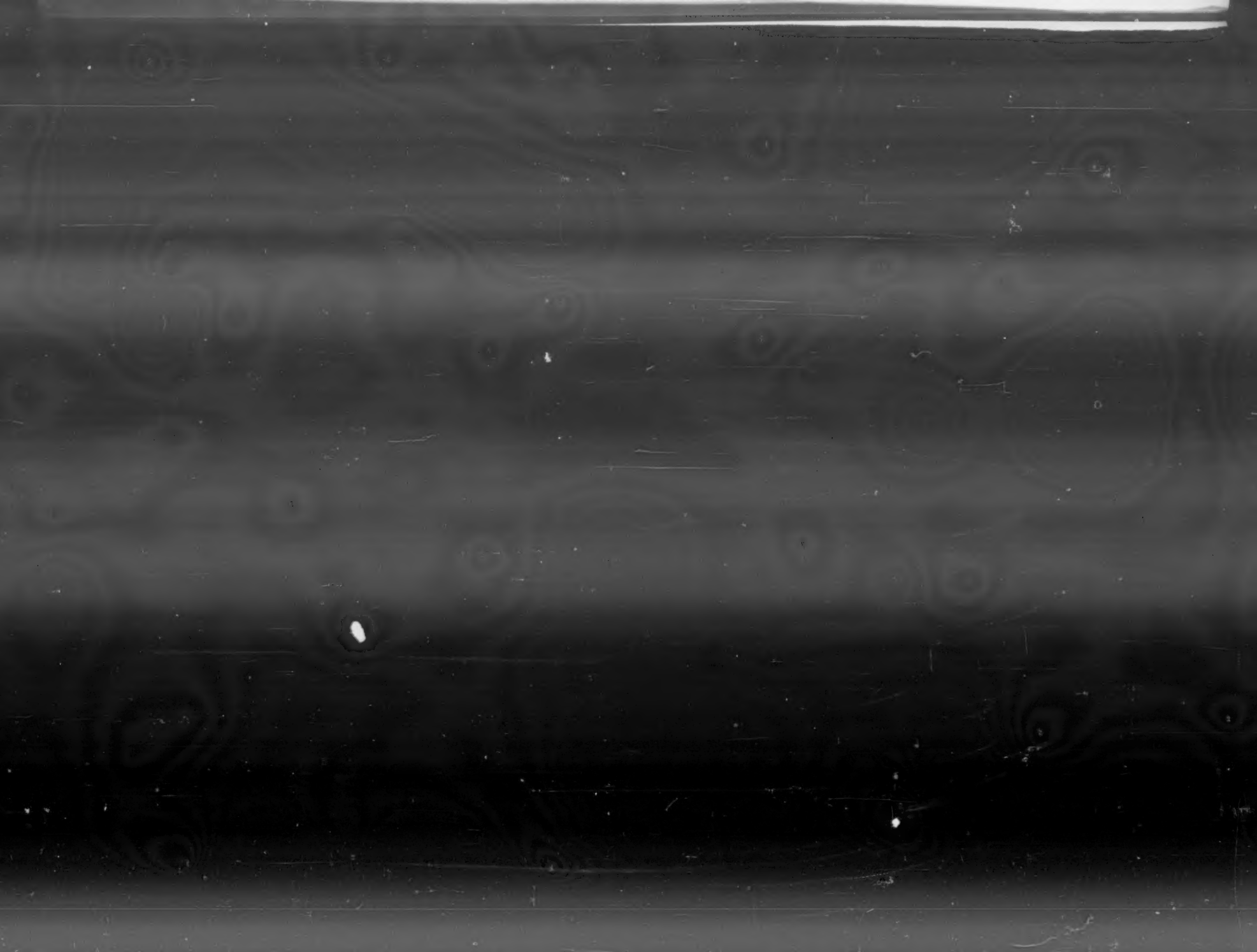

INDEX

Transactions of American Society for Metals

Volume LXI 1968

Index of Authors

A

Aaronson, H. I. 349–351
Abraham, J. K. 233–241
Alden, Thomas H. 559–567
Ansell, G. S. 242–254; 598–604
Antony, K. C. 550–558
Anusavice, K. J. 354–356
Armijo, J. S. 270–277
Aronsson, Bertil 627–629
Asunmaa, S. K. 195–202
Ault R. T. 75–84
Aust, K. T. 270–277

B

Backofen, W. A. 300–313
Balluffi, R. W. ..... 698–699 (A)*

A = abstract only.
Compiled by Mrs. D. Motsch, East Cleveland, Ohio.

Banerjee, B. R. 103–109
Bar-Or, A. 703–710
Barrett, Craig R. ..... 695–697 (A)
Barton, C. J. 635–639
Bartrum, S. F. ..... 646–647 (A)
Beltz, R. J. 790–797
Bennett, J. A. 210–218
Benscoter, A. O. 293–299
Bird, James E. ..... 697–698 (A)
Biss, V. 834–842
Blickwede, D. J. 653–679
Brewer, A. W. 784–789
Breyer, N. N. 219–232
Brophy, J. H. 82–93; 542–549
Brown, Norman ..... 700–701 (A)
Buchwald, J. 750–756

C

Cairns, R. L. 798–806
Chang, W. H. 550–558
Cheng, I-Lin 14–25
Chilton, J. M. 635–639
Clauer, Allan H. ..... 646 (A); 701–702 (A)
Clausing, D. P. 534–541
Coldren, A. P. 834–842
Collins, H. E. 139–148; 711–721
Conrad, H. 847–849
Cooley, L. A. 568–574
Corrie, J. D. 321–329
Cowan, R. L. 3–9
Craig, G. B. 829–833
Craig, J. V. 468–473
Crooker, T. W. 568–574
Cuddy, L. J. ..... 647 (A)
Curtis, R. E. 115–127

D

Davidson, T. E. 242–254
DeAngelis, R. J. 757–768
DeHoff, R. T. 314–320; 354–356
Dorn, John E. ..... 697–698 (A)
Dreshfield, R. L. 352–354; 711–721
Dulis, E. J. 103–109
Duran, S. A. ..... 642–643 (A)
Duquette, D. J. 449–456
Duvall, D. S. 582–591

F

Fager, D. N. 283–292
Field, T. T. 582–591
Flagella, P. N. ..... 646–647 (A)
Flinn, John E. 37–41
Floreen, S. 188–190; 474–488; 489–499
Fraikor, F. J. 784–789
Freed, C. N. 568–574
French, R. D. 190–192

G

Gerberich, W. W. 184–187; 843–847
Gessinger, G. H. 598–604
Gibson, R. C. 85–93
Giessen, Bill C. 330–335
Gilbert, E. R. ..... 642 (A)
Gilman, John J. 861–864
Goldberg, Alfred 26–36
Grant, Nicholas J. 330–335
Gray, J. M. 255–269
Green, J. A. S. 625–627
Griffith, A. A. 871–906
Gschneidner, K. A., Jr. 435–441
Gurland, J. 156–167
Guy, A. G. 110–114; 314–320; 354–356

H

Hahn, G. T. 807–814
Halford, G. R. 94–102
Hartbower, C. E. 184–187
Harvey, M. R. 629–631
Hauser, J. J. 103–109
Hayden, H. W. 85–93; 474–488; 489–499; 542–549
Heckel, R. W. 750–756
Hemmings, P. L. 843–847
Hertzberg, R. W. 769–766
Hinton, R. W. 176–183
Holtman, R. G. 75–84
Hoover, W. R. 769–776
Hyatt, B. 168–175

I

Ingersoll, R. G. 195–202
Inoue, N. 847–849
Itagaki, Motoo 330–335

J

Jackson, J. K. 233–241
Jackson, Ross J. 336–343
Jensen, J. 582–591
Johnston, T. L. 349–351

K

Karchner, G. H. 457–467
Karim, Anwar-Ul ..... 643 (A)
Kasak, A. 10–13
Kear, B. H. 519–527
Kimmel, G. 703–710
Kirkaldy, J. S. 605–619
Koch, E. F. 270–277
Kovach, C. W. 575–581
Krauss, G. 168–175
Kriege, Owen H. 278–282

L

Lake, J. S. H. 829–833
Lange, E. A. 568–574
Lee, D. 742–749
Lenel, F. V. 598–604
Levine, E. 128–138
Li, James C. M. ..... 699–700 (A)
Libsch, J. F. 203–209
Lindborg, U. 500–504
Lindsay, R. W. 790–797
Liu, C. T. 156–167
Lund, J. A. 722–729
Lyne, C. M. 10–13

M

McCoy, H. E., Jr. 730–741
McDonald, John C. 505–518
McElroy, D. L. 730–741
Machlin, E. S. 777–783
Mackay, T. L. 195–202
McMasters, O. D. 435–441
Manson, S. S. 94–102
Marder, A. R. 293–299
Meakin, J. D. 321–329
Merica, P. D. 381–419
Merz, M. D. 843–847
Meyn, D. A. 42–51; 52–61
Miley, Delmar, V. 336–343
Miller, G. A. 442–448
Miller, R. L. 592–597
Montague, W. G. 468–473
Morrison, W. B. 423–434
Moskowitz, A. 575–581
Mostovoy, S. 219–232
Mukherjee, Amiya K. ..... 697–698 (A)
Myers, J. R. 75–84

N

Nehrenberg, A. E. 834–842
Newkirk, John B. 367–372
Nix, William D. ..... 659–697 (A)
Nordberg, Hans 627–629
Norman, E. C. ..... 642–643 (A)
Novick, D. T. 777–783

O

Oblak, J. M. 519–527
Oikawa, Hiroshi 110–114; 354–356

P

Peters, D. T. 62–74
Philofsky, Elliott M. 37–41
Pugh, E. N. 468–473

Q

Queener, C. A. 757–768
Quigg, R. J. 139–148; 711–721

R

Rafalski, A. L. 629–631
Raffo, Peter ..... 645–646 (A)
Rau, R. C. ..... 646–647 (A)
Remy, J.-F. 110–114
Richards, P. N. 528–533
Richman, M. H. 190–192
Riefenberg, D. H. 629–631
Rinnovatore, J. V. 321–329
Risenbrough, N. R. 722–729
Rosen, A. 703–710
Rosenfield, A. R. 807–814
Russell, J. D. 528–533

S

Schaller, F. W. 631–635
Schmatz, D. J. 349–351
Scott, H. 381–419
Sedriks, A. J. 625–627
Seltzer, M. S. ..... 645 (A)
Sheffler, K. D. 203–209
Simcoe, Charles R. 834–842
Slattery, P. W. 625–627
Smith, C. B. 314–320
Snape, E. 631–635
Soderquist, S D. 435–441
Spitzig, W. A. 344–349; 635–639
Spurr, W. F. 115–127; 283–292
Staehle, R. W. 3–9
Stephenson, E. T. 457–467
Sullivan, C. P. 149–155; 278–282; 582–591

T

Thomas, G. 14–25
Tiner, N. A. 195–202
Tomlinson, A. P. 528–533
Townsend, R. D. 605–619
Tuffnell, G. W. 798–806

U

Uhlig, H. H. 449–456

V

Venkatesan, P. S. 620
Votava, E. 807–814

W

Waltenberg, R. G. 381–419
Webster, D. 815–828
Weertman, J. 681–694
Weissmann, S. 128–138
Wells, C. H. 149–155
Wells, R. G. 575–581
Westbrook, J. H. 270–277
Wilcox, B. A. ..... 646 (A)
Williams, J. A. ..... 644–645 (A)
Wilshire, B. ..... 643–644 (A)
Wu, K. C. 621–652

Y

Yeo, R. B. G. 255–269

Z

Zackay, V. F. 843–847
Zehr, S. W. 300–313

A

Aging
effect of stress-corrosion cracking of Ti alloys ... 122–124
of Be sheet ... 786–788
of Fe alloys ... 234–241
of maraging steels ... 802
of Ni superalloys ... 139–148
Alpha brass, 70:30
diffraction patterns ... 324–325
embrittlement ... 327–328
electron microscopy ... 323–324
fracture ... 325–326
Aluminide coatings
on Ni superalloys ... 153–154
Aluminum
defect structure ... 133–136
effect of stress-corrosion cracking of Cu alloys ... 471
fatigue striations ... 128–137
substructure ... 829–833
structure ... 128–137
Aluminum-B composite
ballistic impact ... 556–557
creep properties ... 553–555
fatigue properties ... 555–556
stress calculation ... 559
tensile properties ... 552–553
thermal shock resistance ... 557
Aluminum intermetallic compounds
$AlFeBe_4$ in Be sheet ... 788
AlLi in Mg alloys ... 509–513
Al_3Ni whiskers ... 774–775
ASM Symposium
Dislocation climb and high-temperature creep processes ... 642–647, 680–703
Anisotropy
of graphie in Fe ... 203–209
of sheet steels ... 660–662
Annealing
effect on fracture of stainless steels 486–487
effect of stress-corrosion cracking of Ti alloys ... 120
effect on tensile properties of stainless steels ... 479
of maraging steels ... 802
Annealing twins
in Fe alloys ... 3–4
Ausforming
of martensitic stainless steels ... 817, 821–822
Austenite
determination in textured alloys ... 594
effects in maraging steels ... 799–801
formation in steels ... 349–351
in high speed steels ... 792–797
in maraging steels ... 22
in martensitic stainless steels 816–821; 825–826
in stainless steels ... 490–494
reversion ... 63–73
Austenitic stainless steels
Type 304
chromium-depletion theory ... 275–276
correlation of structure with corrosion ... 271–273
corrosion ... 273–274
microhardness ... 273–274
sequestration of segregate ... 276
tensile properties ... 273
Type HNM
effect of P on $M_{23}C_6$ precipitation. 103–108
structure ... 104–108

B

Bearings
effect of S on fatigue ... 10–13
carbide solution ... 752–753
carbide thickening ... 753–755
cyclic stressing ... 751–752
microstructure ... 11–13; 752–755
Beryllium
grain-size refinement by straining under hydrostatic pressure ... 847–848
Beryllium sheet
aging of quenched specimens ... 786–788
dislocations ... 785–786
precipitation of $AlFeBe_4$ ... 788
precipitation of $FeBe_{11}$ ... 786–788

C

Campbell Memorial Lecture ... 653–679
Carbide precipitates
in austenitic stainless steels ... 103–108
Carbides
in Ni superalloys ... 352–354
Carbon
effect of M_s temperature in Fe alloys 634–635
Cerium
diffusion in Pu alloys ... 629–631
Chromium
effect on Ni superalloys ... 352–354
Chromium-depletion
in austenitic stainless steels ... 275–276
Cooling rates
effect on fracture of stainless steels ... 479–482
effect on tensile properties of stainless steels ... 479
Copper alloys
Cu-Al
effect of Al on stress-corrosion cracking ... 471
stress-corrosion cracking ... 471
Cu-Ni
effect of Ni on stress-corrosion cracking ... 471
Cu-Ni-Zn
diffusion of Zn ... 354–356
Cu-Zn
effect of Zn on stress-corrosion cracking ... 470–471
stress-corrosion cracking ... 469–471
Corrections
The frequency of annealing twins in fcc iron-nickel-chromium alloys ... 853
A microfractographic investigation of fatigue cracks in a low alloy cast steel ... 853
A theoretical explanation for the increase in fatigue strength of mild steel at elevated temperatures ... 192
Corrosion
of austenitic stainless steels ... 271–274
Corrosion fatigue
of steels ... 451–456
Corrosion resistance
of stainless steels ... 89–90

Crack propagation
in Al alloys.....42–50; 52–61; 210–214, 216
in steels.....163–644–645 (A); 808–814
Creep
at high temperatures.....697–698 (A)
deformation.....699–700 (A)
diffusion controlled....642–643 (A); 685–686
effect of order.....700–710 (A)
effect of screw dislocations..... 643 (A)
effect of neutron irradiation..... 642 (A)
failure.....644–645 (A)
in fatigue estimation..... 94–101
in Mo alloys.....645–646 (A)
in Ni alloys...545–549; 643–644 (A); 646 (A)
in stainless steels..... 647 (A)
in W.....646–647 (A)
in Zn alloys..... 728
jog-dragging creep model.....691–692
model..... 642 (A)
of Al composites..... 555–556
of Pb alloys..... 560–562
of PbS..... 645 (A)
of Mo.....701–702 (A)
Creep rate
for subgrains..... 687–689
Crystallographic texture
of sheet steels..... 660–662
of Zr alloys..... 745

D

Diffusion
effect on creep.....642–643 (A)
of Ni into U..... 703–709
of U into Ni..... 703–709
of Zn into Cu alloys..... 354–356
Discussions of
Columbium carbonitride precipitation in low-alloy steels with particular emphasis on "precipitate-row" formation..... 851–852
The interrelation of grain size and superplastic deformation in Ni-Cr-Fe alloys..... 852–853
Properties of stainless steels with a microduplex structure..... 640–641
Some characteristics of aqueous stress-corrosion in titanium alloys. 850–851
A theoretical explanation for the increase in fatigue strength of mild steel at elevated temperatures.... 357–358
Dislocation
climb velocity..... 686–687
glide.....695–697 (A)
mechanisms.....698–699 (A)
substructure.....701–702 (A)
Dislocations
effect on creep..... 643 (A)
in Be sheet..... 785–786
Ductility
effect of pressure on in Fe alloys..... 246–251
of steels..... 162

E

Elasticity
for cubic crystals in the stereographic triangle..... 620
Electrical resistivity
of Ni alloys..... 730–741
Electrolytic separation
of gamma-prime from Ni superalloys 278–282
Electron fractography
of steels..... 569–571
Electron microautography
in microsegregation of H_2 in Ti alloys 195–202
Electron microscopy
in observation of sintering of Ag powders..... 598–604
of alpha brass..... 323–324
of steels.....256; 464–465; 836–840
transverse sectioning of field ion specimens..... 190–192
Embrittlement
of alpha brass..... 327–328
of martensitic stainless steels..... 80–82

F

Fatigue
effect of creep..... 94–101
of Al alloys.42–50; 52–61; 210–218; 774–775
of Al composites..... 555–556
of bearing steels..... 10–13
of steels..... 451–456
Fatigue cracking
of high-strength steels..... 442–447
of maraging steels..... 442–447
of Ni superalloys..... 149–155
Fatigue crack growth
in cast steels..... 627–629
in steels..... 571–573
Fatigue life
of maraging steels..... 178
Fatigue strength
of stainless steels 89
Fatigue striations.....
in Al..... 128–137
Ferrite
in stainless steels..... 490–494
Field ion microscopy
transverse sectioning of specimens for electron microscopy..... 190–192
Flow
classic work by Griffith..... 871–906
commentary on Griffith..... 861–864
Flow stress
in steels..... 536–537
of Ni alloys..... 544–545
Fracture
behavior..... 163–164
effect of pressure..... 246–252
model..... 165–166
of alpha brass..... 325–326
of Al alloys.....43–50; 54–61; 770–775
of cast steels..... 627–629
of pearlite in steels..... 500–504
of stainless steels.....482–488; 494–498
of steels.....156–166; 226–227; 334–349; 465–466; 537–541; 569–571
of Ti alloys.....118–126; 285–289
of TRIP steels..... 845–846
of Zr alloys.....744, 746–748
stress..... 162
Fracture toughness
of high-strength steels..... 446–447
of maraging steels..... 446–447
of martensitic stainless steels.....
.....815–816, 818–821, 825–826
of TRIP steels..... 844–845

G

Gamma-prime, in Ni superalloys
electrolytic separation..... 278–282
formation..... 145–147

Grain shape
analysis in measurement of strain distribution ... 37–41
Grain size
in Pb alloys ... 306–307; 562–564
in maraging steels ... 68
in Ni alloys ... 543–545
in sheet steels ... 659
in steels ... 431–432
of Be ... 847–848
Graphite
anisotropy in Fe ... 203–209

H

Hardness
of Fe alloys ... 234
of maraging steels ... 33–35
of steels ... 256; 460
Heat treatment
of Fe alloys ... 243–244
of maraging steels ... 802
of martensitic stainless steels ... 76–77; 815
of steels ... 256; 458–459
of U alloys ... 336–337
High speed steels
martensite ... 793–796
retained austenite ... 792–797
transformation temperatures ... 792
High-strength steels
4340
fatigue-crack growth rate ... 442–447
fracture toughness ... 446–447
growth-rate dependence on stress intensity, m ... 444–446
H-11
fatigue-crack growth rate ... 442–447
fracture toughness ... 446–447
growth-rate dependence on stress intensity, m ... 444–446
Homogenization
of maraging steels ... 806
Hot working
of maraging steels ... 806
of stainless steels ... 90–92
Hydrogen
in Ti alloys ... 195–202

I

Impact properties
of Fe ... 205–207
of steels ... 460–461
Internal friction
in steel strips ... 532
Iron
behavior in tension ... 206–207
graphite shape anisotropy ... 204–205
impact behavior ... 205–206
mechanical properties ... 205–207
statistical analysis of graphite anisotropy ... 207–209
Iron alloys
Fe-1.39C
microcracking ... 294–298
structure ... 294–298
structure of acicular martensite ... 294–298
Fe-1.86C
microcracking ... 294–298
structure ... 294–298
structure of acicular martensite ... 294–298
Fe-14Cr-4Ni
effect of C on M temperature ... 634–635
M determinations ... 632
M temperatures ... 632–633
Fe-Ni
determination of austenite content 633–66
effect of austenite content on coercive force ... 71–72
effect of austenite on phase diagram 72–73
measurement of coercive force ... 66
Fe-14Cr-4Ni
effects of C on M_s temperature ... 634–635
M_s determinations ... 632
M_s temperatures ... 632–633
Fe-Ni-C
cyclic transformation ... 168–175
effect of structure of properties ... 173–175
fine structure ... 172–173
mechanical properties ... 169–171
structure ... 171
Fe-Ni-C
cyclic transformation ... 168–175
effect of structure on properties ... 173–175
fine structure ... 172–173
mechanical properties ... 169–171
structure ... 171
Fe-Ni-Cr
frequency of annealing twins ... 3–4
structure of system ... 4–6
twinning frequency ... 4–8
Fe-Ni-Co
determination of austenite content 63–66
effect of austenite content of coercive force ... 71–72
effect of Co on austenite ... 73
measurement of coercive force ... 66
Fe-31N-3.5Ti
aging studied by x-ray ... 234–241
hardness studied by x-ray ... 234
precipitation during aging ... 239–241
structure during aging ... 234–241
Iron-carbon alloys
atmospheric pressure mechanical properties ... 245
effect of pressure on elongation ... 248–249, 251
effects of degree of super-saturation ... 618–619
effects of pressure upon macroscopic fracture appearance ... 249–252
effects of pressure upon ductility ... 246–251
evolution of Widmanstätten plates ... 616–618
growth rate of Widmanstätten plates 611–613
heat treatment ... 243–244
high pressure tensile testing ... 245–246
measurements ... 606–608
microstructure ... 608–611
relationship between pressure and true strain to fracture ... 246–248
relationship between pressure coefficient of ductility and strain hardening coefficient ... 251
spacing between Widmanstätten plates ... 613–616
specimen configuration ... 244

L

Lanthanum-lead system
intermetallic compounds of system ... 437–440
inverse peritectic and eutectic reactions ... 436–437
phase diagram ... 436
thermal analysis ... 435–436
x-ray and metallographic methods ... 436

Lead
effect on mechanical properties of steels ... 227–232
Lead alloys
Pb-5% Cd
activation energy ... 564
activation energy for superplastic creep ... 562
creep ... 560–562
effect of grain size ... 562–564
mechanism of superplasticity ... 564–566
microstructure ... 560
strain hardening ... 560–562
Pb-Sn
as-extruded eutectic ... 303–304
creep viscosities ... 306
extruded and annealed eutectic ... 304
grain size and temperature effect ... 306–307
mechanical properties ... 303–308
metallographic changes ... 308–311
metallography ... 302–303
strain-rate hardening ... 308–311
superplasticity ... 303–312
tensile testing ... 301–302
Lead sulfides
effect of stoichiometric defects on creep ... 645 (A)
Liquid metal embrittlement
in steels ... 228–231
Loop fracture test
in steel strips ... 528–529
Low-alloy steels
banding and grain size ... 431–432
effect of alloying elements ... 432–434
microstructure ... 428–431
strain-rate sensitivity ... 427–428
superplasticity ... 423–434
tensile tests ... 424–426

M

Magnesium alloys
LA141A
precipitation and reversion of theta 506–509
precipitation of AlLi ... 509–513
strength and formability ... 514–516
Maraging steels
250 grade
determination of austenite content 66
effect of austenite composition ... 67–68
effect of austenite content on coercive force ... 71–72
effect of grain size ... 68
effect of Mo and Ti on austenite ... 73
effect of prior exposure ... 68–71
measurement of coercive force ... 66
300 grade
effect of thermal cycling on dilatometric heating ... 27–31
effect of thermal cycling on hardness ... 33–35
effect of thermal cycling on microstructure ... 31–33
effect of thermal cycling on x-ray diffraction ... 31–33
strengthening mechanisms ... 637–639
structure ... 637–639
350 grade
alloy rebalancing ... 799–801
ausaging ... 805–806
development ... 798–806
effect of aging ... 802
effect of annealing ... 802
effect of test temperature ... 802–804
effects of increased hardner content 798–799
heat treatment ... 802
homogenization and hot workability ... 806
M_s and austenite effects ... 799–801
properties of a 5000-lb heat ... 801–802
properties of sheet and wire ... 804–805
weldability ... 806
12Ni-5Cr-3Mo
cyclic hardening ... 178–179, 181
fatigue life ... 178
stress relaxation ... 177–180
substructure developed by fatigue 181–183
18 Ni
fatigue-crack growth rate ... 442–447
fracture toughness ... 446–447
growth-rate dependence on stress intensity ... 444–446
20Ni-23Co-0.07Al-0.17Ti
as-quenched state ... 15–16
martensitic grain size ... 24
mechanical properties ... 16–17; 22–23
ordering ... 24
precipitate dispersion ... 24
precipitate identification ... 17–21
precipitate morphology ... 22
reversion of austenite ... 22
strength ... 23–24
structural changes ... 22–23
transformation temperature ... 15
Martensite
acicular ... 294–298
grain size ... 24
Martensitic stainless steels
AFC 77
ausforming ... 817
calculation of the critical carbide size of cause cleavage in the surrounding ferrite ... 828
control and determination of retained austenite content ... 816–821
effect of austenitizing temperature ... 826
effect of low temperature testing ... 826
effect of tempering temperature for specimens austenitized at 2000 F 825–826
fracture toughness testing ... 815–816, 825–826
heat treatment ... 815
microstructure stability at elevated temperatures ... 825
nature of embrittlement ... 80–82
properties of ausformed material ... 821–822
properties of strain aged material 821–825
selection of heat treatment for minimizing delta ferrite content 76–77
strain aging ... 817
strength ... 77–78
stress-corrosion cracking ... 78–80
stress-corrosion testing ... 816, 826–827
tension and compression ... 816
toughness ... 77–78
transverse mechanical properties ... 821
Metallurgical Classics
Heat treatment and constitution of duralumin ... 381–419
The phenomena of rupture and flow in solids ... 861–906
Microstructure
of bearing steels ... 11–13
of Fe alloys ... 608–611
of Pb alloys ... 560

of maraging steels 31–33
of martensitic stainless steels 825
of steel bearings 752–755
of steels 428–431; 462–465; 836–840
of Ti alloys 622–624
of W ..... 646–647 (A)
Molybdenum
dislocation substructure formed during creep ..... 701–702 (A)
effect of maraging steels 73
effect of Ni superalloys 352–354
Molybdenum alloys
Mo-Ti-C
creep ..... 645–646 (A)
dynamic strain aging ..... 645–646 (A)

N

Neutron irradiation
effect on creep ..... 642 (A)
Nickel
effect on stress-corrosion cracking of Cu alloys 471
Nickel alloys
calculation of fringe profiles 524–526
dynamical theory of fringe contrast. 519–520
electrical resistivity 732–741
fringe profiles 526
geometrical model for fringe contrast 519
Nimonic 80A
creep resistance ..... 643–644 (A)
Ni-Al
effects of experimental variables in etching 586–588
potentiostatically controlled etching 582–591
Ni-Cr
creep ..... 646 (A)
Ni-20% Cr
creep resistance ..... 643–644 (A)
Ni-Cr-Fe
creep 548–549
dislocations 546–549
effect of deformation on grain size 543–544
effect of grain size on flow stress ... 544–545
effect of second-phase particle distribution on grain size 543–544
stress relaxation 545–546
superplasticity 546–549
Nickel superalloys
B-1900
effect of aging on γ' formation 145–146
effect of aging on minor phases 141, 144–145
structure 143–148
IN-100
effect of aging on γ' formation 145–146
effect of aging on minor phases 140, 143–145
structure 143–148
Rene 41
effect of aging on γ' formation 146–147
effect of aging on minor phases 142, 144–145
structure 143–148
U-700
effect of aging on γ' formation 146–147
effect of aging on minor phases 144
structure 143–148
Udimet 700
effect of aluminide coatings on crack initiation 153–154
electrolytic separation of γ' 278–282
low-cycle fatigue crack initiation .. 149–155
Unitemp AF2-1D
effect of aging on γ' formation 146–147
effect of aging on minor phases 142, 145
structure 143–148
VI A
alloy formation 714–717
properties 717–719
statistical designs 711–714
Niobium carbonitride
precipitation in steels 263–268

P

Pearlite
fracture in steels 500–504
in steels 808–814
structure of fracture in steels 503–504
Phase changes 684
in creep 684
Phase diagrams
of Fe-Ni alloys 72–73
of La-Pb system 436
Phase susceptibilities
of Ti alloys 285–286
Phosphorus
effect on $M_{23}C_6$ precipitation in austenitic stainless steels 103–108
Plutonium alloys
Pu-Ce
Ce diffusion 629–631
Precipitation
dispersion in maraging steels 24
in Be sheet 786–788
in Mg alloys 506–513
in maraging steels 17–21
in steels 256–268
of Fe alloys 239–241
structure in maraging steels 22
Prestressing
of Al alloys 214–215

R

Rhenium
effect on solid solubility of W alloys 779–782

S

Sintering
of Ag powders 598–604
Sodium amalgams
effect of embrittlement of alpha brass 327–328
Sodium chloride
effect of fatigue of steels 451–456
Solid phases
in steels 578–580
Solid solubility
of Al alloys 330–335
of O_2 in W 779
of O_2 in W alloys 779–782
Springback
derivation of equation 767–768
determination 758, 760–761
Stainless steels
corrosion resistance 89–90
fatigue strength 89
hot workability 90–92
room-temperature strength 86–89
room-temperature toughness 86–89
structure 85–92
superplasticity 85–86

Type 304
effect of substructure on creep.... 647 (A)
18-8
toughness..... 188–190
25% Cr – 6% Ni
effects of composition on properties 498–499
fracture..... 494–498
tensile behavior of ferrite and austenite..... 490–494
tensile behavior of tie-line heats... 494
26% Cr – 6.5% Ni
compositional effects..... 484–486
effects of annealing treatments on tensile properties..... 479
effect of cooling rate on fracture.. 479–482
effect of cooling rate on tensile properties..... 479
effect of test temperature and strain rate on tensile properties. 477–478
effects of annealing treatments on fracture..... 486–487
fracture appearances.....482–484, 487–488
orientation effects..... 478–479
work hardening..... 475–477
Statistics
in development of Ni superalloys.... 711–721
Steady-state creep..... 681–685
activation energy..... 683
activation volume..... 683–684
effect of phase change..... 684
isotope effect..... 684
position in creep diagram..... 682
relation between dislocation glide and recovery.....659–697 (A)
stress dependence 684–685
unlimited creep strain..... 681–682
Steels
5LX52
microcrack morphology..... 808–810
pearlite structure..... 808–814
relation between slip lines and microcracks..... 810–813
1015
appearance of initial cracks..... 453
effect of O_2 on fatigue..... 451–456
effect of NaCl on fatigue..... 451–456
4145
atom transport..... 231
effect of Pb on mechanical properties..... 227–232
fractography..... 226–227
impact tests..... 224–226
liquid metal embrittlement..... 228–229
tensile tests..... 222–224
D6aC
dimple size..... 184–186
stress fracture..... 184–186
0.02C – 0.50Mn – 0.10Nb
electron microscopy..... 256
hardness..... 256
heat treatment..... 256
precipitate formation..... 256–268
precipitation of niobium carbonitride..... 263–268
structure..... 256–268
transformation..... 256–263
0.030% C – 0.072% Mn – 1.46% Ni – 0.93% Cr – 1.54% Mo – 2.29% W – 0.57% V
electron microscopy..... 836–840
mechanical properties.....835–836, 841
microstructure..... 836–841
0.17% Cr – 0.39% Mn – 0.01% P – 0.04% S
cleavage fracture..... 537–538
effect of strain on specimen geometry..... 537
effect of temperature on flow stress 536–537
fibrous fracture..... 540
fracture data..... 537
fracture locus..... 539–540
tensile tests..... 535–536
0.45 C – Ni – Cr – Mo
crack-opening displacement..... 348–349
plain-strain fracture..... 344–349
process zone size..... 347–348
Fe 13 Cr – Mn – S
liquidus surface..... 577–578
solid phase relationships..... 578–580
sulfide phases..... 575–581
0.5% Mo – B – V
electron microstructure and diffraction..... 462–465
fracture..... 465–466
hardness..... 460
heat treatment..... 458–459
impact properties..... 460–461
metallography..... 459
tensile properties..... 460
9 Ni – 4 Co – 0.25 C
electron fractography..... 571
fatigue crack growth..... 571–573
fracture mechanics..... 569–571
Strain aging
effect of C and N..... 673–674
in sheet steels..... 672–676
of martensitic stainless steels.....817, 821–825
of Mo alloys.....645–646 (A)
Strain distribution
analysis of boundary shape..... 37–38
determination..... 37–41
measuring local changes in grain shape..... 37–41
Strain hardening
in Fe alloys..... 251
of Pb alloys..... 560–562
Strain-rate hardening
of Pb alloys..... 308–311
of sheet steels..... 658–659
Strain rates
effect on tensile properties of stainless steels..... 477–478
of steels..... 427–428
of TRIP steels..... 845
of Zn..... 723–724
of Zr alloys..... 749
Straining
of Be under hydrostatic pressure.... 847–848
Stress
calculation of in Al composites..... 559
Stress-corrosion
of martensitic stainless steels....816, 826–872
Stress-corrosion cracking
of Cu..... 469
of Cu alloys..... 468–473
of martensitic stainless steels..... 78–80
of Ti alloys.....120–124; 285–291
Structure
effect of composition and processing of sheet steels..... 666–672
effect of heating rate..... 669–670
of Al.....128–137; 829–833
of austenitic stainless steels..104–108; 271–273
of cold-worked steels..... 662–664
of Fe alloys.....4–6; 171–175; 234–241; 294–298
of maraging steels..21–22; 181–183; 637–639
of Ni superalloys..... 143–148

of pearlite fracture in steels..... 503–504
of sheet steels..... 662–665
of stainless steels.....85–92; 647 (A)
of steels..... 256–268
of Ti alloys.....118–125; 285–289
of U alloys..... 339–343
Subgrain creep..... 686
Sulfide phases
of steels..... 575–581
Sulfur
effect on fatigue of bearing steels.... 10–13
Superplasticity
of Pb alloys.....303–312; 564–566
of Ni alloys..... 546–549
of stainless steels..... 85–86
of steels..... 423–434
Supersaturation
of Al alloys..... 330–335
of Fe alloys..... 618–619

T

Tensile properties
of Al alloys..... 770
of Al composites..... 552–553
of austenitic stainless steels..... 273
of stainless steels.....477–479; 490–494
of steels..... 460
of Ti alloys..... 118–122
of U alloys.....337–339, 341–342
of Zr alloys..... 745–749
Tensile tests
of alpha brass..... 322, 324
of Fe alloys..... 245–246
of Pb alloys..... 301–302
of steels.....222–224; 424–426; 535–536
of Ti alloys..... 116–117
Texture
effect of alloying elements..... 667–668
effect of composition and grain size.. 668–669
of cold-worked steels..... 662–664
of sheet steels..... 662–665
Textured alloys
determination of retained austenite.. 594
volume fraction analysis of phases.. 592–597
x-ray diffraction..... 592–597
Titanium
effect of maraging steels..... 73
failure in methanol-HCl-H_2O solutions..... 625–626
Titanium alloys
efficiency of emulsions..... 197–199
examination of microautoradiographs 199–202
introduction of radioactive H_2..... 195–196
microsegregation of H_2 by electron microautoradiography..... 195–202
preparation of microautoradiographs 196–197
Ti – 4 Al – 3 Mo – 1V
cracking characteristics.....285–289, 291
effect of aging on stress-corrosion cracking..... 122–124
effect of annealing on stress-corrosion resistance..... 120
effect of prior β treatment on stress-corrosion cracking.....120–122
effect of prior β treatment on tensile properties..... 120–122
effect of solution temperature on fracture and tensile properties 118–120
fracture plane orientation..... 286–288
fracture tests..... 116–117
phase susceptibilities..... 285–286
structure..... 118–125
tensile tests..... 116–117
thickness effect..... 288–289
Ti – 5 Al – 25 Sn
cracking characteristics.....285–289, 291
fracture plane orientation..... 286–288
phase susceptibilities..... 285–286
thickness effect..... 288–289
Ti – 6 Al – 4 V
cracking characteristics.....285–289, 291
effect of aging on stress-corrosion cracking..... 122–124
effect of annealing on stress-corrosion resistance..... 120
effect of prior β treatment on stress-corrosion cracking..... 120–122
effect of prior β treatment on tensile properties..... 120–122
effect of solution temperature on fracture and tensile properties 118–120
fracture plane orientation..... 286–288
fracture tests..... 116–117
phase susceptibilities..... 285–286
structure..... 118–125
tensile tests..... 116–117
thickness effect..... 288–289
Ti – 8 Al – 1 Mo – 1 V
continuous-cooling transformation diagrams..... 621–624
cracking characteristics.....285–289, 291
fracture plane orientation..... 286–288
microstructure..... 622–624
phase susceptibilities..... 285–286
thickness effect..... 288–289
Ti – 13 V – 11 Cr – 3 Al
cracking characteristics..... 289–291
Torsion
of Al alloys..... 210–216
Toughness
of martensitic stainless steels..... 77–78
of stainless steels.....86–89; 188–190
Transformation
in steels..... 256–268
Tungsten
creep.....646–647 (A)
effect of Ni superalloys..... 352–354
microstructure.....646–647 (A)
solid solubility of O_2..... 779
Tungsten alloys
W-1¼ at. % Re
bright spot concentration..... 779–782
effect of Re on lattice solid solubility of O_2..... 779–782
W-3 at. % Re
bright spot concentration..... 779–782
effect of Re on lattice solid solubility of O_2..... 779–782

U

Uranium alloys
U-Nb
heat treating..... 336–337
metallographic and x-ray studies.. 339–343
structure..... 339–343
tensile properties.....337–339, 341–342
Uranium intermetallic compounds
formed during interdiffusion between U and Ni..... 705–707

W

Widmanstätten plates
evolution in Fe alloys..... 616–618

growth in Fe alloys..... 611–613
spacing in Fe alloys..... 613–616

X

X-ray analysis
of aging in Fe alloys..... 233–241
of La-Pb system..... 436
of U alloys..... 339–343
X-ray diffraction
in determination of volume fraction analysis of textured alloys..... 592–597
of maraging steels..... 31–33
of steels..... 462–464

Z

Zinc
diffusion of in Cu alloys..... 354–356
effect on stress-corrosion cracking of Cu alloys..... 470–471
strain rate..... 723–724
Zinc alloys
Zn-Ni-Ti
creep at 100 C..... 728
deformation..... 722–729
tensile characteristics..... 724–728
Zircalloy-2
crystallographic texture..... 745
fracture strain and fractography.. 744
mechanical testing..... 744
pole figure determination..... 743
room temperature and 350 C strain to fracture..... 746–748
room temperature strength..... 745–746
strain rate effect at 350 C..... 749
tensile properties..... 745–749